nature neuroscience

Allosteric potentiation of glycine receptor chloride currents by glutamate

Jun Liu[1,3], Dong Chuan Wu[1–3] & Yu Tian Wang[1,2]

Neuronal excitability in the CNS is primarily controlled by a balance between synaptic excitation and inhibition. In the brainstem and spinal cord, synaptic excitation and inhibition are mediated by the excitatory transmitter glutamate acting on ionotropic glutamate receptor–gated cationic channels and the inhibitory transmitter glycine acting on glycine receptor (GlyR)-gated chloride channels. We found that glutamate and its analog ligands potentiated GlyR-mediated currents in both cultured spinal neurons and spinal cord slices of rats. This potentiation was not dependent on activation of any known glutamate receptor and manifested as an increase in single-channel open probability. Moreover, this glutamate potentiation was seen in HEK293 cells that transiently expressed GlyRs. Our data strongly suggest that glutamate allosterically potentiates GlyR-gated chloride channels, thereby blurring the traditional distinction between excitatory and inhibitory transmitters. Such a rapid homeostatic regulatory mechanism may be important for tuning functional balance between synaptic excitation and inhibition in the CNS.

Neuronal excitability is fundamental to neuronal function and is primarily controlled by a fine balance between synaptic excitation and inhibition. In the mammalian CNS, synaptic excitation is chiefly mediated by the excitatory transmitter glutamate acting on ionotropic glutamate receptor–gated cationic channels and synaptic inhibition is primarily mediated by the inhibitory transmitter GABA acting on the $GABA_A$ receptor–gated chloride channel[1]. In contrast, synaptic inhibition in the brainstem and spinal cord is principally mediated by glycine acting on the glycine receptor (GlyR)-gated chloride channel[2,3]. However, in addition to being a primary inhibitory transmitter, glycine can also contribute to excitatory transmission by serving as an allosteric modulator for the NMDA receptor (NMDAR)[4–6].

We found that glutamate and its ligand analogs allosterically potentiated GlyR-mediated currents by interacting with a binding site that is probably on the α subunit of GlyRs. Along with previously demonstrated glycine potentiation of excitatory NMDA receptors[4], our findings not only blur the traditional distinction between an excitatory and an inhibitory transmitter system, but also lead us to propose a new model of functional cross-talk between the two classical fast transmitters via the reciprocal allosteric enhancement of each other's receptor function. This reciprocal modulation between the two classic excitatory and inhibitory transmitter systems could act as a rapid homeostatic control mechanism for neuronal excitability.

RESULTS

AP5 potentiates glycinergic mIPSCs in spinal neurons

We carried out whole-cell patch-clamp recordings on cultured spinal neurons. Miniature postsynaptic events were recorded at −60 mV in the presence of the voltage-gated sodium channel blocker tetrodotoxin (TTX, 0.5 μM) and the $GABA_A$ receptor antagonist bicuculline (10 μM). The synaptic events can be characterized into two major populations on the basis of their kinetics: a fast population, which had a mean 10–90% rising time of 0.77 ms ± 0.06 and a decay time constant (τ_D) of 4.8 ± 0.90 ms, and a slow population, which had a mean 10–90% rising time of 1.55 ± 0.3 ms and a τ_D of 14.7 ± 3.0 ms (**Fig. 1a**). On the basis of these kinetics, the fast population likely represents miniature excitatory postsynaptic currents (mEPSCs) mediated by glutamate acting on cationic ion channels, whereas the slow population likely represents GlyR-mediated miniature inhibitory postsynaptic currents (mIPSCs)[7,8]. To isolate mIPSCs from mEPSCs, we sequentially applied the AMPA receptor (AMPAR) antagonist 6-cyano-7-nitroquinoxaline-2,3-dione (CNQX) and the NMDAR antagonist D(−)-2-amino-5-phosphonovaleric acid (AP5) in the extracellular perfusion solution.

As expected, CNQX (10 μM) selectively abolished events with fast kinetics (**Fig. 1b**), confirming that the fast synaptic events are mEPSCs mediated by AMPARs[7]. Subsequent perfusion of AP5 (100 μM) resulted in a marked increase in the amplitude of remaining slow synaptic events (**Fig. 1c**). These remaining synaptic events were indeed glycinergic mIPSCs, as they were abolished by bath application of the GlyR antagonist strychnine (1 μM; **Fig. 1d**). This AP5 potentiation was reversible, as mIPSCs recovered to the control level after AP5 washout (**Fig. 1e**). AP5 increased the amplitude of glycinergic mIPSCs (137.4 ± 10.1% of the control, $P < 0.05$, $n = 7$) without affecting their frequency (control, 0.53 ± 0.21; AP5, 0.56 ± 0.19 Hz; $P > 0.05$, $n = 7$) (**Fig. 1f,g**). We analyzed the rising and decay time courses of mIPSCs (**Fig. 1h**) and found that AP5 had little effect on 10–90% rising time (control, 1.55 ± 0.3 ms; AP5, 1.49 ± 0.4 ms) or τ_D (control, 14.7 ± 3.0 ms; AP5, 16.2 ± 3.9 ms). The decay phase of averaged mIPSC was best fitted with single-exponential function (**Fig. 1h**). The selective enhancement

[1]Brain Research Centre and Department of Medicine, Vancouver Coastal Health Research Institute, University of British Columbia, Vancouver, British Columbia, Canada. [2]Translational Medicine Research Center and Center for Neuropsychiatry and Graduate Institute for Immunology, China Medical University Hospital, Taichung, Taiwan. [3]These authors contributed equally to this work. Correspondence should be addressed to Y.T.W. (ytwang@interchange.ubc.ca).

Received 2 June; accepted 13 August; published online 12 September 2010; doi:10.1038/nn.2633

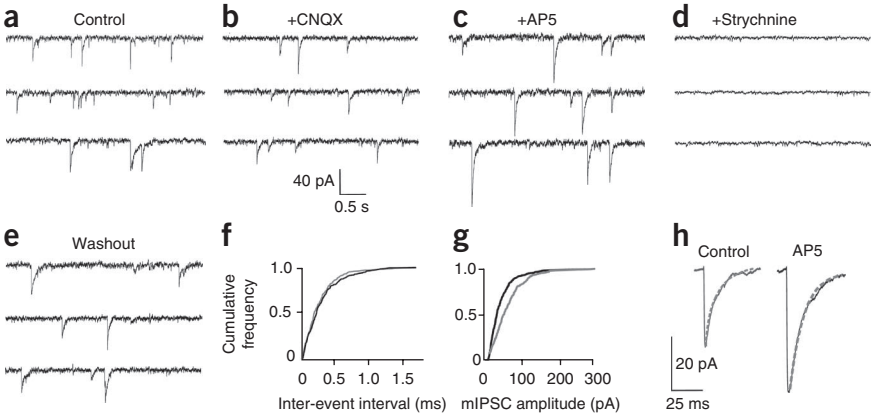

Figure 1 AP5 potentiates glycinergic mIPSCs. (**a**–**e**) Whole-cell patch-clamping of cultured spinal neurons were performed at a holding potential of −60mV. Glycinergic mIPSCs were isolated by addition of 0.5 μM TTX and 10 μM bicuculline (**a**), 10 μM CNQX (**b**) and 100 μM AP5 (**c**). AP5 produced a reversible increase in the mIPSC amplitude without affecting its frequency, which was reversibly blocked by 1 μM strychnine. (**f**,**g**) Cumulative frequency and amplitude distribution histograms of mIPSCs from the same cell before (control, black line) and after addition of AP5 (gray line). (**h**) Traces averaged from 100 individual mIPSCs before and after AP5 application indicate that AP5 had no effect on mIPSC kinetics. The decay phase of averaged mIPSC was best fitted with the single-exponential function (dotted lines). The rising time and τ_D were 1.6 ms and 14.8 ms in control and 1.4 ms and 15.4 ms after AP5, respectively.

of the amplitude of mIPSCs without altering their frequency and kinetics strongly suggests that this potentiation is most likely mediated by AP5 acting via a postsynaptic mechanism.

Potentiation of glycine currents by glutamate analogs

To further confirm the postsynaptic locus of the modulation, we investigated the effect of AP5 on postsynaptic GlyR-mediated currents evoked by pressure ejection of glycine from a micropipette near the recorded neurons in the presence of TTX, CNQX and bicuculline (**Fig. 2**). Under these conditions, the glycine current was blocked by bath application of 1 μM strychnine, confirming that the currents were strychnine-sensitive, GlyR-mediated chloride currents. Consistent with postsynaptic modulation, bath application of AP5 (50 μM) caused a reversible increase in glycine currents (138.1 ± 12.2% of the control, $P < 0.01$, $n = 6$; **Fig. 2a**,**e**).

The potentiated glycine currents induced by AP5 may be a result of the blockade of an ambient glutamate activation of NMDAR-mediated inhibition of GlyR function. If this is the case, we would expect that direct activation of NMDARs by bath application of NMDA should inhibit the GlyR-mediated currents. To our surprise, application of NMDA (50 μM) in the absence of extracellular Mg^{2+} produced an even greater potentiation of glycine currents (180.2 ± 13.3% of the control, $P < 0.01$, $n = 6$; **Fig. 2b**,**e**).

The qualitatively similar potentiation of glycine currents by both AP5 and NMDA strongly suggests that the potentiation is not dependent on activation of NMDA receptors. This conjecture was further tested by blocking NMDAR channels with MK-801, a use-dependent noncompetitive NMDAR antagonist[9]. To fully block NMDAR channels, we first applied MK-801 (10 μM) with NMDA (50 μM) in the Mg^{2+}-free extracellular solution. NMDA-induced currents were progressively and completely inhibited by MK-801 (**Fig. 2c**). The MK-801 blockade of NMDA channels was irreversible, as applying NMDA (50 μM) after MK-801 washout failed to produce any observable current (**Fig. 2c**). When we blocked NMDAR channels with MK801, NMDA-induced potentiation of glycine currents largely remained (147.7 ± 14.6% of the control, $n = 5$, $P < 0.01$; **Fig. 2c**,**e**). These results indicate that the potentiation does not require the opening of NMDAR channels.

However, it remains possible that the potentiation is mediated by the binding of NMDA or AP5 to the glutamate-binding site on the

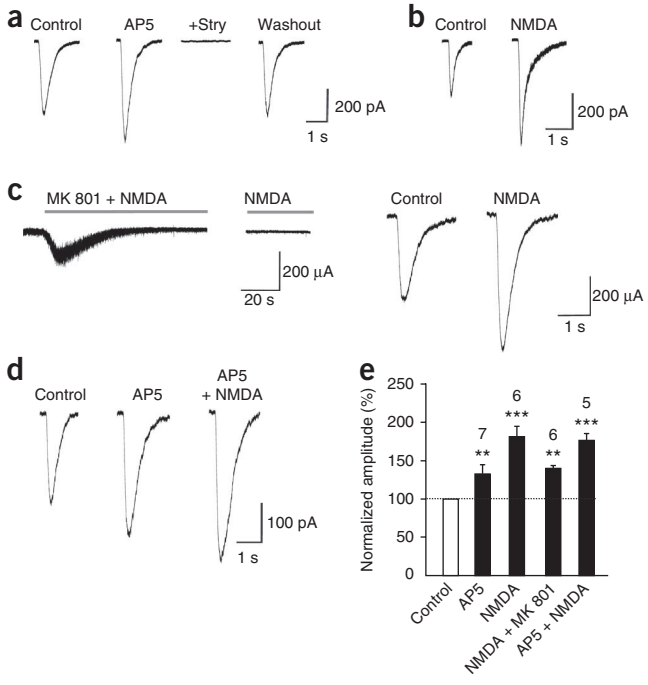

Figure 2 AP5 and NMDA potentiate GlyR-mediated currents via a NMDAR-independent mechanism. (**a**) AP5 reversibly potentiated postsynaptic glycine-induced currents evoked by pressure ejection of glycine (100 μM) from a pipette positioned close to the recorded cells. Representative current traces were obtained under control conditions, 1 min after application AP5 (50 μM) or strychnine (+Stry, 1 μM), and 2 min after AP5 and strychnine were washed out. (**b**) NMDA potentiated glycine-induced currents. Representative traces were obtained in the absence (control) and presence of NMDA (50 μM) in Mg^{2+}-free extracellular solution. (**c**) NMDA-induced potentiation did not require the opening of NMDAR-gated channels. Blockade of NMDA channels was produced by coapplication of NMDA (50 μM) and MK-801 (10 μM) (left) and subsequent application of NMDA did not alter the holding current (middle). Right, representative glycine-evoked currents obtained before (control) and after application of NMDA (50 μM) following the NMDAR blockade. The extracellular solution contained 1.3 mM Ca^{2+} and 0 mM Mg^{2+}. (**d**) AP5 (50 μM) and NMDA (50 μM) produced greater potentiation of glycine currents than AP5 alone. The extracellular solution contained 1 mM Mg^{2+}, 0 mM Ca^{2+} and 5 mM EGTA. (**e**) Bar graph summarizing the data from **a**–**d** showing the effects of AP5 and/or NMDA on glycine-induced currents under various conditions. The number of cells in each group is indicated on the top of each bar. Error bars indicate s.e.m. $^{**}P < 0.01$ and $^{***}P < 0.001$.

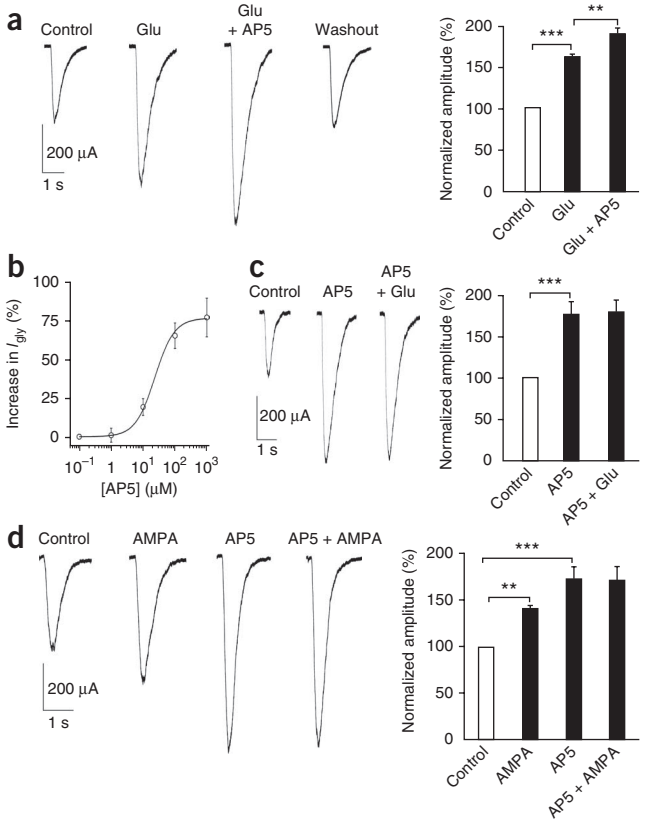

Figure 3 Potentiation of GlyR-mediated currents by glutamate ligands in cultured spinal neurons. Whole-cell currents evoked by glycine (100 μM) were recorded with the intracellular solution supplemented with 20 mM BAPTA and in the presence of CNQX (20 μM to block AMPARs and KARs), MK-801 (10 μM to block NMDARs), YM-298198 (10 μM to block mGluR1) and MPEP (10 μM to block mGluR5) in 5 mM EGTA and Ca^{2+}-free and extracellular solution. (**a**) Glutamate (Glu, 50 μM) reversibly potentiated glycine currents and AP5 potentiation was additive to glutamate-induced potentiation (Glu + AP5, $n = 7$). (**b**) Dose-response curve for AP5-induced potentiation of glycine currents ($n = 6$). All values are expressed as a percentage increase of glycine-evoked current (I_{gly}). Each data point is the mean ± s.e.m. of glycine currents at the indicated AP5 concentrations compared with glycine response (control). The solid line is the best fit of the data to the Hill equation, which yields a mean EC_{50} of 49.4 ± 7.60 μM and Hill coefficient of 1.86. (**c**) AP5 at the saturating concentration (1 mM) resulted in a pronounced potentiation of the glycine current and occluded further potentiation by glutamate (50 μM), as quantified in the graph on the right ($n = 5$ for each group). (**d**) AMPA (50 μM) potentiated glycine-induced currents and the potentiation was occluded by the potentiation induced with the saturating concentration of AP5 (1 mM) ($n = 6$ for both groups). Error bars indicate s.e.m. $^{**}P < 0.01$ and $^{***}P < 0.001$.

NMDARs without activation of the receptor channels. We hypothesized that if the potentiation requires that NMDA occupies the ligand-binding sites of NMDARs in the absence of channel activation, AP5 should occlude NMDA potentiation by competing for the same ligand-binding site. Bath application of AP5 (50 μM) alone increased the glycine-induced current to 134.2 ± 11% of the control ($n = 7$, $P < 0.01$; **Fig. 2d**). However, in contrast with our expectation, AP5 failed to occlude NMDA-induced potentiation of glycine currents. In fact, NMDA (50 μM) in the presence of AP5 resulted in a greater enhancement of the glycine current (176 ± 7.8%, $n = 6$, $P < 0.001$; **Fig. 2d**). The potentiation of glycine currents caused by NMDA and AP5 was significantly different from that induced by AP5 alone ($P < 0.01$, $n = 5$; **Fig. 2d**,**e**). These results strongly suggest that NMDA and AP5 may potentiate GlyR-mediated currents, not by acting on the NMDAR glutamate-binding site, but by a previously unknown glutamate-binding site.

These observations prompted us to test whether the potentiation can be mimicked by other known glutamate ligands, such as the endogenous ligand glutamate itself or AMPA, a selective ligand that specifically binds to the AMPAR. Glutamate is an endogenous excitatory neurotransmitter acting through both ionotropic (AMPA, NMDA and kainate receptor subtypes) and metabotropic glutamate receptors (mGluRs) in the CNS[10–12]. mGluRs are further classified into eight subtypes ($mGluR_{1\text{-}8}$), of which $mGluR_1$ and $mGluR_5$ are mainly located on postsynaptic sites[13]. To determine whether glutamate mimics NMDA and AP5 in potentiating glycine currents via a previously unknown binding site, we applied glutamate in the presence of CNQX (20 μM, to block AMPA and kainate glutamate receptors), MK-801 (10 μM, to block NMDARs), YM-298198 (10 μM, to block $mGluR_1$ receptors) and MPEP (2-methyl-6-(phenylethynyl)pyridine hydrochloride, 10 μM, to block $mGluR_5$ receptors). Under these conditions, glutamate (50 μM), similar to NMDA or AP5, produced a reversible increase in the glycine current (161.2 ± 26.7%, $n = 7$, $P < 0.001$; **Fig. 3a**). Coapplication of AP5 (50 μM) and glutamate did not prevent glutamate-induced potentiation, but instead resulted in a greater potentiation (200.3 ± 16.6%, $n = 5$, $P < 0.01$; **Fig. 3a**) than that produced by glutamate alone. To determine whether glutamate exerts its effect via the same binding site as AP5, we performed occlusion experiments. We assumed that if two ligands compete for the same acting site, a saturating concentration of AP5 should be sufficient to occlude the glutamate effect. We first determined the dose-response relationship of AP5-induced potentiation on glycine currents. AP5 potentiation occurred in a dose-dependent manner with a half maximal effective concentration (EC_{50}) at 49.4 ± 7.6 μM and saturating concentration of about 1 mM (**Fig. 3b**). At the saturating concentration (1 mM), AP5 induced a marked potentiation of the glycine current and this potentiation was not further increased by the subsequent addition of glutamate (50 μM; **Fig. 3c**). This suggests that glutamate and AP5 act on the same binding site in potentiating glycine currents. Similar to glutamate, application of AMPA (50 μM) also resulted in a significant potentiation of glycine currents (141.3 ± 7.4%, $n = 7$, $P < 0.01$; **Fig. 3d**) and this potentiation was occluded by the potentiation produced with a saturating concentration of AP5 (**Fig. 3d**). Together, these results strongly suggest that these glutamate ligands share a glutamate-binding site, likely on GlyRs.

AP5 increases GlyR single-channel open probability

Next, we explored the mechanisms underlying potentiation of GlyR function using single-channel recordings under both outside-out and on-cell attached configurations (**Figs. 4** and **5**). We used AP5 as the glutamate-like ligand in these experiments to avoid potential complications as a result of the activation of any ionotropic glutamate receptor–gated channel activities. In outside-out patches held at −60 mV, bath application of glycine (5 μM) evoked single-channel activities, as previously reported[14,15], which were composed of several conductances (**Fig. 4a**). The most frequent conductance states consisted of the main (38.5 ± 4.3 pS) and one evident subconductance (25.2 ± 3.4 pS) ($n = 6$; **Fig. 4b**,**d**). Application of AP5 (50 μM) to the patch did not produce any single-channel activity on its own (data not shown), but instead substantially increased glycine-induced single-channel activities. We found that AP5 significantly increased the overall frequency of single-channel events (control, 0.88 ± 0.16 Hz; AP5, 1.16 ± 0.23 Hz; $P < 0.05$,

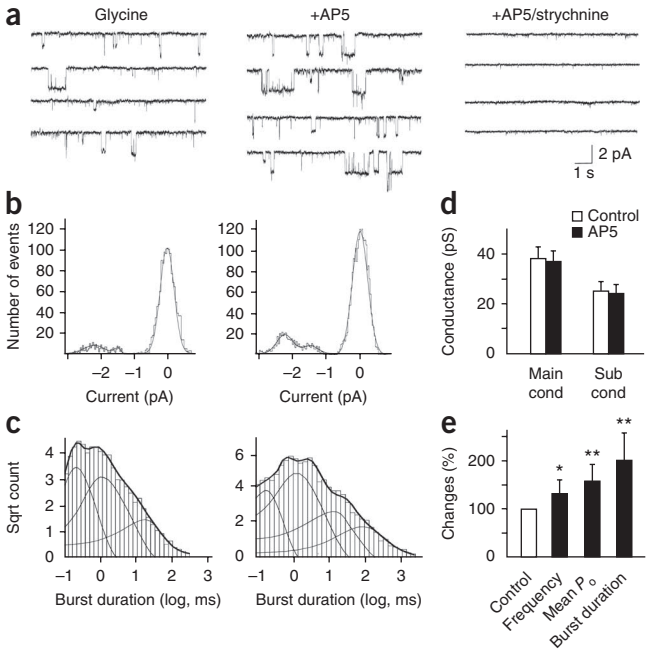

Figure 4 AP5 increases GlyR-mediated single-channel activities in the outside-out mode. (**a**) Glycine-induced single-channel activity was increased by AP5 in outside-out patches. Glycine (5 μM), AP5 (50 μM) and strychnine (1 μM) were applied to the patches through bath applications. Representative current traces were obtained in the absence of AP5 (glycine), in the presence of AP5, and in the presence of AP5 and strychnine at a holding potential of –60 mV. AP5 increased the single-channel activity, which was blocked by strychnine. (**b**) Amplitude histograms before and after AP5 application from the same patch. Single-channel currents before and after AP5 application were best fitted with two Gaussian distributions and AP5 had little effect on either main or subconductance. (**c**) Representative burst-duration histograms before and after AP5 application. Distributions were fitted by the sum of three and four exponential components (thinner lines) before (control) and after AP5. The thicker line is a fit of all of the data. (**d**) Bar graphs pooled from six patches showing no changes in the main and subconductances before (control) and after AP5. (**e**) Bar graphs summarizing changes in frequency, mean open probability (P_o) and burst duration before (control) and after AP5. Error bars indicate s.e.m. $^*P < 0.05$ and $^{**}P < 0.01$.

$n = 6$; **Fig. 4e**) and open probability (P_o; control, 0.06 ± 0.03; AP5, 0.12 ± 0.04; $P < 0.01$, $n = 6$; **Fig. 4e**). AP5 had little effect on the main (37.3 ± 3.9 pS, $P > 0.05$) and subconductance (24.2 ± 3.2 pS, $P > 0.05$) (**Fig. 4b**,**d**). We analyzed the kinetic properties of channel openings in bursts. In the absence of AP5, the single-channel burst duration histogram was best fitted with the sum of three exponentials (glycine alone; **Fig. 4c**). The mean time constants were 0.34 ± 0.16 ms (τ_1), 1.68 ± 0.24 ms (τ_2) and 20.7 ± 0.8 ms (τ_3), with the mean burst duration being 9.7 ± 2.5 ms (**Fig. 4c**). After AP5 application, however, the burst duration histogram was fitted with the sum of four exponential components (τ_1, 0.27 ± 0.15 ms; τ_2, 1.41 ± 0.33 ms; τ_3, 22.5 ± 1.3 ms; τ_4, 119.7 ± 21.6 ms), with the mean burst duration being 15.2 ± 3.4 ms (**Fig. 4c**), which was significantly different from that of the control ($P < 0.01$, $n = 6$; **Fig. 4e**). The increased mean burst duration was primarily a result of the occurrence of the fourth component following AP5 application, as statistical analysis showed that AP5 had no substantial influence on the first three components.

The observation that potentiation can be detected in the outside-out patch strongly suggests that the putative glutamate-binding site responsible for the potentiation is either on the GlyR itself, or on an unidentified glutamate-binding receptor/protein closely associated with the GlyR. This is more clearly demonstrated by single-channel recordings under the on-cell attached configuration (**Fig. 5**). In these recordings, glycine (5 μM) was included in recording pipettes filled

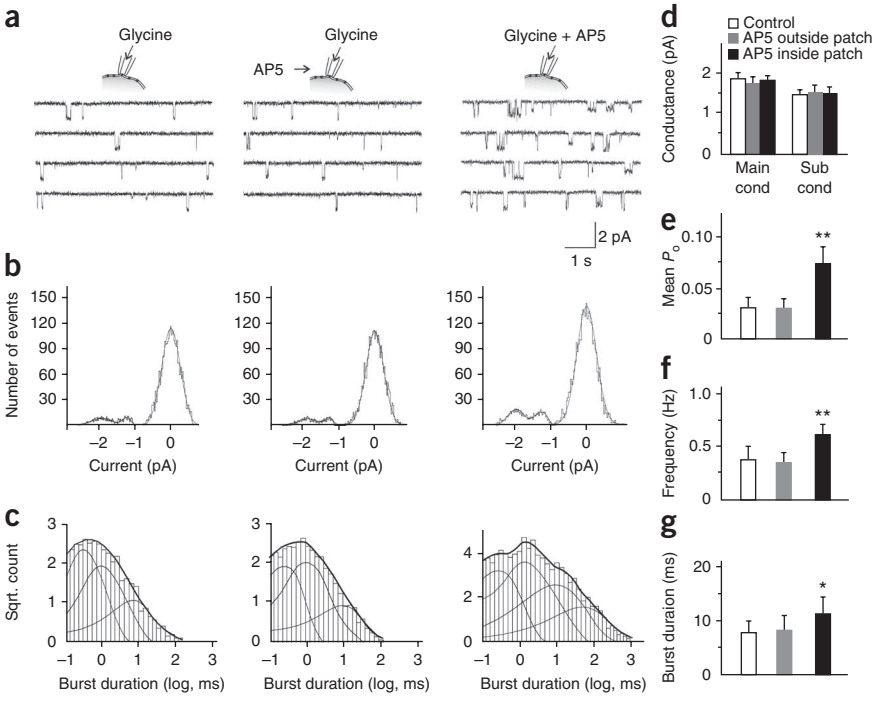

Figure 5 AP5 increases GlyR-mediated single-channel activities in the on-attached mode. (**a**) Effects of AP5 on glycine-induced single-channel currents. As illustrated in the diagrams above the representative continuous current traces, single-channel activities were evoked by 5 μM glycine applied inside of the patch alone (left), with AP5 (50 μM) applied outside of the patch (middle) or with AP5 (50 μM) applied inside of the patch (right). The single-channel activity was only increased by AP5 applied through the recording pipette (right). (**b**) Representative amplitude histograms from the same patches in **a** showing that single-channel currents were best fitted with two component Gaussian distributions and that AP5 applied either outside or inside of the patches did not alter either main or subconductances. (**c**) Representative burst-duration histograms from patches in **a**. The burst distributions were fitted by the sum of three exponential components (thinner lines) in control (left) and AP5 applied outside of the patch (middle), but were fitted by the sum of four exponential components when AP5 was applied inside the patch (right). The thicker line is a fit of all of the data. (**d**–**g**) Bar graphs pooled from seven patches showing the single-channel conductances (cond; **d**), frequency (**e**), burst duration (**f**) and P_o (**g**) in controls and in AP5 applied outside ($n = 7$) or inside of the patches ($n = 6$). Error bars indicate s.e.m. $^*P < 0.05$ and $^{**}P < 0.01$.

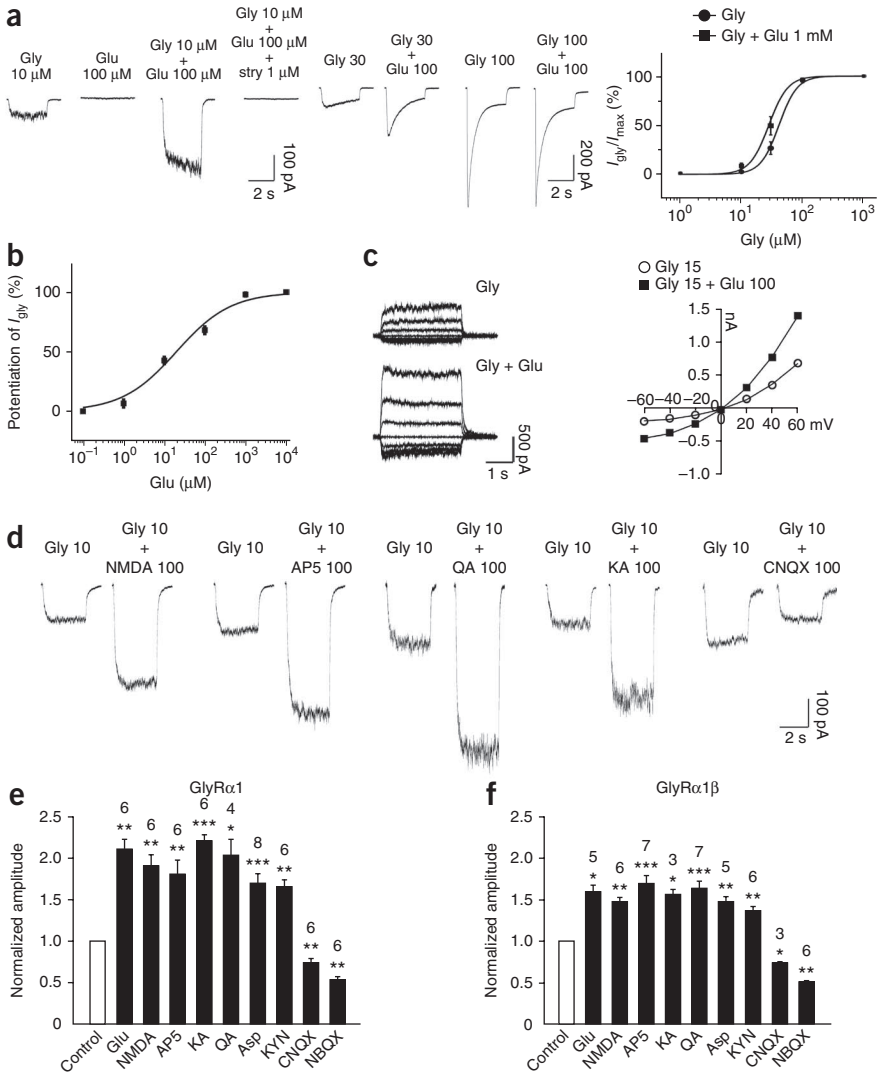

Figure 6 Glutamate-like ligands potentiate recombinant GlyR function. (**a**–**f**) HEK293 cells were transiently transfected with human α1 (**a**–**e**) or α1β (**f**) subunits. (**a**) Representative traces showing glutamate potentiation of glycine currents in a dose-dependent manner. Glutamate (Glu, 100 μM) alone produced no detectable currents, but instead potentiated glycine currents that were blocked by 1 μM strychnine. Right, glycine dose-response curves in the absence (Gly) and presence (Gly + Glu 1mM) of glutamate ($n = 6$). (**b**) Dose-response curve of glutamate-induced potentiation of glycine-induced (10 μM) currents (I_{gly}, $n = 9$). (**c**) Glutamate potentiation of glycine currents is not associated with alteration of the reversal potential. Left, representative glycine-induced (15 μM) current traces at various holding potentials in the absence (Gly) and presence of glutamate (100 μM; Gly+Glu). Right, current-voltage (*I-V*) relationship curves showing that glutamate potentiation was not associated with an alteration of the reverse potential. (**d**) Effects of glutamate-like ligands on glycine-induced currents. Representative traces show the effects on glycine-induced (10 μM) currents of 100 μM NMDA, AP5, quisqualate (QA), kainic acid (KA) and CNXQ. (**e**,**f**) Bar graphs summarizing the effects of various glutamate ligands on the glycine currents recorded from homomeric α1 (**e**) and heteromeric α1β (**f**) GlyRs. All glutamate-like ligands were applied at 100 μM, except for kynurenic acid (1 mM, KYN) and NBQX (10 μM). The number of cells in each group is indicated at the top of each bar. Error bars indicate s.e.m. $^*P < 0.05$, $^{**}P < 0.01$ and $^{***}P < 0.001$.

with the extracellular solution at a pipette potential (V_p) of 0 mV (**Fig. 5a**). Under the control condition, glycine-induced single-channel currents had two evident conductance states (**Fig. 5a**,**b**,**d**) with the mean P_o being 0.03 ± 0.01 ($n = 7$; **Fig. 5e**). The burst duration histogram was best fitted with the sum of three exponential components (τ_1, 0.28 ± 0.13; τ_2, 1.47 ± 0.29 ms; τ_3, 18.4 ± 0.6 ms) with the mean burst duration being 8.2 ± 2.1 ms ($n = 7$; **Fig. 5c**). When AP5 (50 μM) was applied to the outside of the recording pipette, it had little effect on P_o, single-channel conductances or other single-channel properties (**Fig. 5**). However, when coapplied with glycine to the inside of the recording pipette, AP5 significantly increased both the frequency ($P < 0.01$, $n = 6$; **Fig. 5f**) and mean P_o ($P < 0.01$, $n = 6$; **Fig. 5e**) without affecting single-channel conductances (**Fig. 5b**,**d**). Similar to the observation in the outside-out mode, the burst duration histogram was best fitted with the sum of four exponential components (τ_1, 0.24 ± 0.15 ms; τ_2, 1.38 ± 0.27 ms; τ_3, 20.5 ± 1.8 ms; τ_4, 98.7 ± 14.3 ms) in the presence of AP5 (**Fig. 5c**). The mean burst duration was increased to 11.4 ± 3.2 ms from 8.2 ± 2.1 ms ($P < 0.05$, $n = 6$; **Fig. 5g**), which appeared to primarily be the result of the occurrence of fourth component following AP5 application.

Glutamate potentiates recombinant GlyRs in HEK293 cells

To further differentiate whether glutamate potentiation is mediated through the ligand binding to the GlyR or to a closely associated glutamate receptor/protein, we examined the potential regulation of GlyR function in HEK293 cells that transiently expressed recombinant human GlyRs. Functional GlyRs are pentameric channel complexes formed from various subunit combinations of four different α subunits and one β subunit[2,3]. The α subunits can efficiently form functional homomeric GlyRs in recombinant expression systems, although the majority of native GlyRs in the CNS are believed to be heteromeric α1 and β receptors[2]. Therefore, we transiently expressed either recombinant human homomeric α1 (**Fig. 6a**–**e**) or heteromeric α1β GlyRs (**Fig. 6f**) in HEK293 cells. In whole-cell recordings, 10–100 μM glycine produced inward currents in a dose-dependent manner (**Fig. 6a**) and these currents were blocked by 1 μM strychnine (data not shown). Glutamate (100 μM) itself produced no detectable currents, indicating that these cells did not express a functional ionotropic glutamate receptor (**Fig. 6a**). However, co-perfusion of glycine (10 μM) and glutamate (100 μM) caused a significant increase in the peak amplitude compared with glycine alone (glycine alone, −503 ± 156 pA; glycine and glutamate, −1,095 ± 357 pA; $P < 0.01$, $n = 6$, **Fig. 6a**). The potentiation was blocked by 1 μM strychnine (**Fig. 6a**), indicating that the currents are gated through strychnine-sensitive GlyR-gated chloride channels. Glutamate potentiation was glycine concentration dependent, being more pronounced when the currents were induced at lower concentrations and diminished at the saturating concentration of glycine (**Fig. 6a**). Glutamate left-shifted the glycine dose-response curve and reduced the glycine EC_{50} from 40.8 μM to 27.8 μM ($P < 0.05$, $n = 6$) without changing the Hill coefficient. Glutamate potentiation

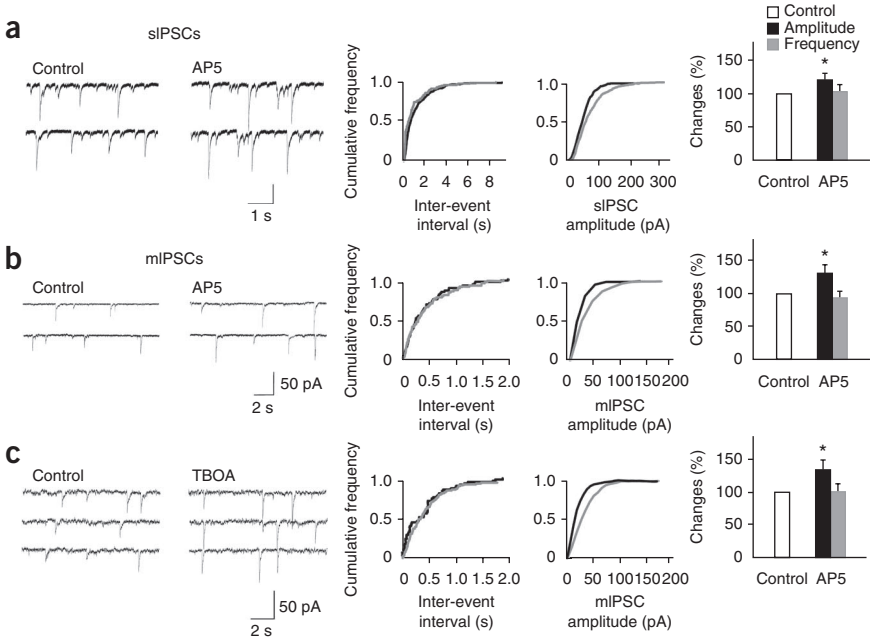

Figure 7 Glutamate potentiation of GlyR-mediated IPSCs in laminae I-II neurons in spinal cord slices. (**a**) AP5 potentiated GlyR-mediated sIPSCs recorded under whole-cell voltage-clamp mode at a holding potential of –65 mV. Left, representative traces of glycinergic sIPSCs before (Control) and after AP5 (AP5; 100 μM) application. AP5 caused a significant increase in the sIPSC amplitude without altering its frequency, as shown in the cumulative frequency and amplitude distribution histograms (middle). Right, bar graphs showing average effects of AP5 on sIPSC amplitude and frequency from six cells before (control) and after AP5 application. (**b**) AP5 potentiated GlyR-mediated mIPSCs. Left, representative traces of glycinergic mIPSCs before (control) and after AP5 (100 μM) application. AP5 caused a significant increase in the mIPSC amplitude without changing its frequency, as shown by the cumulative frequency and amplitude distribution histograms (middle). Right, bar graphs showing average effects of AP5 on mIPSC amplitude and frequency from five cells. (**c**) Inhibition of glutamate transporter activity potentiated GlyR-mediated mIPSCs. Left, representative recordings of mIPSCs before (control) and after application of the glutamate transporter blocker TBOA (10 μM). TBOA caused a significant increase in the mIPSC amplitude without changing its frequency, as illustrated in the cumulative frequency and amplitude distribution histograms (middle). Right, bar graphs showing the average effects of TBOA on mIPSC amplitude and frequency from six cells. Error bars indicate s.e.m. $^*P < 0.05$.

of glycine currents was also dose dependent (**Fig. 6b**). Potentiation was observed in the low micromolar range (~5 μM) with an EC_{50} of 19.9 μM and a saturating concentration of 1 mM.

To determine whether glutamate potentiation of glycine currents is a result of alteration of the chloride equilibrium potential, we examined the current-voltage (*I-V*) relationship by recording glycine currents at various holding potentials before and after bath application of glutamate. Glutamate (100 μM) markedly increased the slope of the *I-V* curve without altering the reversal potential (**Fig. 6c**). This result is consistent with the idea that glutamate potentiation of glycine currents is achieved by modulating GlyR channel function, but not by an alteration in chloride driving force.

To further examine whether glutamate potentiation of glycine currents could be mimicked by other glutamate-like ligands, we tested the effects of various subtype ionotropic glutamate receptor agonists, including NMDA (100 μM), aspartate (100 μM for NMDARs), quisqualate (100 μM for AMPARs) and kainic acid (100 μM for KARs), and antagonists, including NMDAR antagonist AP5 (100 μM), AMPAR and KAR antagonists CNQX (100 μM) and 6-nitro-2,3-dioxo-1,4-dihydrobenzo[f]quinoxaline-7-sulfonamide (NBQX, 10 μM), and the nonselective ionotropic glutamate receptor antagonist kynurenic acid (1 mM). None of these ligands generated detectable currents on their own (data not shown), but all of them (with the exception of CNQX and NBQX) mimicked the action of glutamate, resulting in a significant enhancement of glycine-induced currents ($P < 0.05$; **Fig. 6d**,**e**). The potentiation was qualitatively similar for cells expressing either homomeric α1 (**Fig. 6e**) or heteromeric α1β (**Fig. 6f**) GlyRs, although it appeared to be more pronounced in cells expressing homomeric α1 GlyRs. In contrast with all of the other glutamate-like ligands that we tested, CNQX had little effect on glycine currents at a concentration below 20 μM (data not shown), but at 100 μM it reduced the peak amplitude by 26.6 ± 5.0% ($n = 6$; **Fig. 6d**,**e**) in cells expressing homomeric α1 GlyRs and 26.2 ± 2.2% ($n = 3$) in cells expressing heteromeric α1β GlyRs (**Fig. 6f**). Indeed, CNQX at 100 μM also reduced the amplitude of GlyR-mediated mIPSCs to 71.2 ± 8.6% of the control in cultured spinal neurons ($P < 0.05$, $n = 5$). The CNQX inhibition of glycine currents was mimicked by NBQX in HEK cells (**Fig. 6e**,**f**). Notably, CNQX not only inhibited glycine currents, but also significantly reduced glutamate (20 μM) potentiation (1.70 ± 0.11– and 1.19 ± 0.04–fold potentiation in the absence and presence of 100 μM CNQX, $P < 0.01$, $n = 6$). The results indicate that CNQX and glutamate might act on the same site on GlyRs.

Potentiation of GlyR-mediated IPSCs in spinal cord slices

Together, our results strongly suggest that GlyRs undergo positive allosteric modulation by glutamate-like ligands in both cultured neurons and HEK cells expressing recombinant GlyRs. However, the physiological relevance of this modulation would largely be dependent on whether the modulation occurs in mature neurons in a neuronal network *in situ*. Therefore, we investigated whether glutamate-like ligands can potentiate GlyR-mediated spontaneous IPSCs (sIPSCs) and mIPSCs in acute rat spinal cord slices. We used AP5 instead of glutamate in these experiments to minimize any potential effects from known glutamate receptors. GlyR-mediated sIPSCs were recorded at 22–24 °C in the presence of CNQX (10 μM), MK-801 (15 μM) and bicuculline (10 μM) and in the absence of TTX (**Fig. 7a**). Bath application of AP5 (100 μM) significantly increased the sIPSC amplitude to 131.5 ± 8.2% of the control (control, –36.6 ± 3.4 pA; AP5, –48.1 ± 5.3 pA; $P < 0.05$, $n = 6$; **Fig. 7a**), although it had little effect on sIPSC frequency (control, 1.36 ± 0.2 Hz; AP5, 1.43 ± 0.3 Hz; $P > 0.05$, $n = 6$; **Fig. 7a**). Both basal and potentiated sIPSCs were abolished by 1 μM strychnine (data not shown), confirming the potentiation of GlyR-mediated sIPSCs by AP5. A similar potentiation of sIPSCs by AP5 was also observed when the slices were perfused at a more physiological temperature (30–32 °C). At this temperature, bath application of AP5 increased the sIPSC amplitude to 128.6 ± 6.3% of control

(control, 44.2 ± 10.2 pA; AP5, 56.8 ± 7.4 pA; $P < 0.05$, $n = 5$) without significantly altering sIPSC frequency (control, 2.2 ± 0.4; AP5, 2.5 ± 0.5 Hz; $P > 0.05$).

Next, we investigated the effect of AP5 on GlyR-mediated mIPSCs recorded in the presence of TTX (0.5 μM). Under the control condition, the basal peak amplitude and frequency of mIPSCs were 41.6 ± 6.2 pA and 0.24 ± 0.12 Hz, respectively. AP5 (100 μM) increased the mIPSC amplitude to 136.5 ± 12.4% of the control (56.8 ± 8.7 pA, $P < 0.05$, $n = 5$; **Fig. 7b**) without altering its frequency (0.26 ± 0.13 Hz, $P > 0.05$, $n = 5$; **Fig. 7b**). Finally, we sought to investigate whether the AP5 potentiation of GlyR-mediated inhibitory synaptic transmission can be mimicked by endogenous glutamate. This was done by increasing the concentration of endogenous glutamate following blockade of glutamate transporter activity. We blocked known glutamate receptors with a cocktail of glutamate receptor antagonists (Online Methods). After a stable recording was established, TBOA (DL-threo-b-benzyloxyaspartic acid, 10 μM) was perfused in the extracellular solution. TBOA, similar to AP5, induced in a significant increase in the mIPSC amplitude without altering its frequency (**Fig. 7c**). The mean amplitude of mIPSCs was potentiated to 142.2 ± 15.8% of the control (control, 33.7 ± 3.5 pA; TBOA, 47.9 ± 5.0 pA; $n = 6$, $P < 0.01$;, **Fig. 7c**), whereas the mean frequency of mIPSCs remained largely unchanged (control, 0.32 ± 0.13 Hz; TBOA, 0.35 ± 0.15 Hz; $P > 0.05$, $n = 6$; **Fig. 7c**). This potentiation is likely a result of inhibition of glutamate transporter activity, as TBOA at this concentration had no effect on glycine currents in HEK293 cells expressing recombinant α1/β glycine receptors (data not shown). The kinetic characteristics of glycinergic sIPSC and mIPSCs were also analyzed before and after application of AP5 or TBOA. Statistical analysis revealed no significant differences in 10–90% rising time and τ_D before and after application of AP5 or TBOA ($P > 0.05$).

DISCUSSION

Our results reveal a previously unrecognized positive modulation of GlyR function by various glutamate-like ligands. The demonstration of potentiation using either outside-out patches or on-cell attached recordings when AP5 was applied with glycine into the recording pipette is consistent with an allosteric modulation resulting from a direct binding of glutamate ligands to GlyRs. This was further supported by the similar modulation observed in HEK293 cells transiently expressing recombinant GlyRs, but not glutamate receptors. The observation that the glutamate potentiation can be mimicked by most ionotropic glutamate receptor ligands tested suggests that this putative glutamate-binding site on the GlyR has a distinct pharmacological profile and appears to be less stringent than any glutamate-binding site on known ionotropic glutamate subtype receptors. However, it is interesting to note that CNQX and NBQX, unlike all of the other glutamate-like ligands that we tested, had no positive modulation, but instead had an inhibitory effect on the GlyR-mediated currents. This suggests that the glutamate-binding site has a pharmacological profile that is distinct from other known glutamate-binding sites and such a distinctive profile may allow for the future development of agonists and/or antagonists that can specifically modulate the strength of glycine receptor–mediated synaptic inhibition. This glutamate allosteric regulation of GlyR function is also mechanistically and functionally distinct from the previously reported modulation of GlyRs by glutamate or NMDA[16,17], as this modulation does not require activation of another receptor (AMPA or NMDA receptors) or depend on any diffusible intracellular components[18]. Notably, a previous study found a similar glutamate potentiation of $GABA_A$ receptors[19]. Although it is possible that a known glutamate receptor expressed by these neurons had a modulatory effect, these findings suggest that the glutamate allosteric modulation of GlyR that we found may be extended to other inhibitory chloride channels.

Glutamate and glycine are the primary excitatory and inhibitory transmitters in the mammalian brainstem and spinal cord, respectively. However, the allosteric potentiation of GlyRs by glutamate that we found, along with the previously discovered allosteric potentiation of NMDA subtype of glutamate receptors by glycine[4–6], blurs the classic distinction between excitatory and inhibitory neurotransmitters. These positive cross-talks between glutamate and glycine transmitter systems may also suggest an efficient mode of homeostatic regulation of neuronal excitability via a reciprocal allosteric enhancement of each other's receptor function. The ability of AP5 to potentiate both glycinergic sIPSCs and mIPSCs in the dorsal horn neurons of spinal cord slices strongly suggests that the observed glutamate allosteric modulation of synaptic transmission at glycinergic synapses can take place as long as the glutamate levels surrounding the synapses reaches the required concentrations. It is important to note that the EC_{50} of glutamate modulation of GlyRs that we observed was around 20 μM, which is much higher than basal levels of extracellular glutamate[20,21]. However, extracellular glutamate concentrations can be increased under certain conditions, such as following glutamate uptake inhibition, or under certain physiological and pathological conditions.

The higher EC_{50} than the normal extracellular glutamate concentration also suggests specific physiological and/or pathological importance of the glutamate homeostatic regulation of GlyRs. For example, efficient glial and/or parasynaptic neuronal glutamate transporters will keep presynaptically released glutamate concentrated at synaptic clefts of excitatory synapses under normal conditions, thereby ensuring that glutamate spill-over to adjacent glycinergic synapses occurs at concentrations below the threshold required to potentiate GlyR function. Therefore, under these basal physiological conditions, glutamate primarily functions as an excitatory transmitter, mediating just synaptic excitation. However, under other conditions, such as high-frequency stimulation of presynaptic inputs and/or uncontrolled seizure activity and spastic hypertonia, repetitive firing of glutamatergic neurons leads to excessive accumulation of presynaptically released glutamate to surpass the uptake ability of glutamate transporters, thereby allowing it to transiently escaping uptake and spill-over to the adjacent glycinergic synapses[22–24]. When such a heterosynaptic glutamate spill-over increases glutamate concentrations at nearby glycinergic synapses to the level of a few micromolar, only then will glutamate allosterically potentiate GlyR function, thereby strengthening glycine-mediated synaptic inhibition at these synapses. The enhanced inhibition may, in turn, rapidly and efficiently counteract glutamate-mediated excitation to ensure tight control of neuronal excitability under most physiological conditions. Vice versa, a similar heterosynaptic spill-over feedback mechanism can also take place via glycine potentiation of NMDARs when glycinergic neurons are firing extensively. Compared with other levels of homeostastic regulation, such as neuronal networks[25] or synaptic homeostasis[26,27], this glutamate-glycine reciprocal receptor cross-talk mode is clearly much faster. Such a rapid mode of homeostatic regulation may be particularly important for some neuronal functions that require very tight timing of inputs, such as during synaptic plasticity or rhythmic generations. To this end, it is relevant to note that NMDAR-mediated excitation and glycine-mediated inhibition are thought to be the primary counteracting systems critically involved in the generation and maintenance of the rhythmicity of local motor activity in the spinal cord[28]. Such cross-talk may also be important under certain pathological conditions. For instance, following neurotrauma, the excessive

release of glutamate in combination with compromised glutamate uptake may transiently increase extracellular glutamate concentration to a level of hundreds of micromoles or even millimoles[29–31]. This increased glutamate may in turn potentiate GlyR-mediated chloride conductance, thereby protecting neurons from excessive glutamate-induced excitotoxic neuronal death.

METHODS

Methods and any associated references are available in the online version of the paper at http://www.nature.com/natureneuroscience/.

ACKNOWLEDGMENTS

We thank Y.P. Li for preparation and maintenance of spinal cord neuronal cultures and L. Oschipok for his excellent editorial assistance. This work was supported by the Canadian Institutes for Health Research, the Heart and Stroke Foundation of British Columbia and Yukon, and the Taiwan Department of Health Clinical Trial and Research Center of Excellence (DOH99-TD-B-111-004). J.L. was supported by postdoctoral fellowships from National Sciences and Engineering Research Council, the Michael Smith Foundation for Health Research and the British Columbia Epilepsy Society. Y.T.W. is a Howard Hughes Medical Institute International Scholar and the holder of the Heart and Stroke Foundation of British Columbia and Yukon chair in stroke research.

AUTHOR CONTRIBUTIONS

J.L., D.C.W. and Y.T.W. designed the experiments. J.L. performed and analyzed the experiments in cultured spinal neurons and spinal cord slices. D.C.W. performed and analyzed the experiments in HEK293 cells. J.L., D.C.W. and Y.T.W. wrote the manuscript.

COMPETING FINANCIAL INTERESTS

The authors declare no competing financial interests.

Published online at http://www.nature.com/natureneuroscience/.
Reprints and permissions information is available online at http://www.nature.com/reprintsandpermissions/.

1. Mody, I., De Koninck, Y., Otis, T.S. & Soltesz, I. Bridging the cleft at GABA synapses in the brain. *Trends Neurosci.* **17**, 517–525 (1994).
2. Betz, H. & Laube, B. Glycine receptors: recent insights into their structural organization and functional diversity. *J. Neurochem.* **97**, 1600–1610 (2006).
3. Lynch, J.W. Molecular structure and function of the glycine receptor chloride channel. *Physiol. Rev.* **84**, 1051–1095 (2004).
4. Johnson, J.W. & Ascher, P. Glycine potentiates the NMDA response in cultured mouse brain neurons. *Nature* **325**, 529–531 (1987).
5. Kleckner, N.W. & Dingledine, R. Requirement for glycine in activation of NMDA-receptors expressed in *Xenopus* oocytes. *Science* **241**, 835–837 (1988).
6. Dingledine, R., Kleckner, N.W. & McBain, C.J. The glycine coagonist site of the NMDA receptor. *Adv. Exp. Med. Biol.* **268**, 17–26 (1990).
7. O'Brien, R.J. *et al.* The development of excitatory synapses in cultured spinal neurons. *J. Neurosci.* **17**, 7339–7350 (1997).
8. Keller, A.F., Coull, J.A., Chery, N., Poisbeau, P. & De Koninck, Y. Region-specific developmental specialization of GABA-glycine cosynapses in laminas I-II of the rat spinal dorsal horn. *J. Neurosci.* **21**, 7871–7880 (2001).
9. Wong, E.H. *et al.* The anticonvulsant MK-801 is a potent *N*-methyl-D-aspartate antagonist. *Proc. Natl. Acad. Sci. USA* **83**, 7104–7108 (1986).
10. Mayer, M.L. & Armstrong, N. Structure and function of glutamate receptor ion channels. *Annu. Rev. Physiol.* **66**, 161–181 (2004).
11. Dingledine, R., Borges, K., Bowie, D. & Traynelis, S.F. The glutamate receptor ion channels. *Pharmacol. Rev.* **51**, 7–61 (1999).
12. Collingridge, G.L., Isaac, J.T. & Wang, Y.T. Receptor trafficking and synaptic plasticity. *Nat. Rev. Neurosci.* **5**, 952–962 (2004).
13. Conn, P.J. & Pin, J.P. Pharmacology and functions of metabotropic glutamate receptors. *Annu. Rev. Pharmacol. Toxicol.* **37**, 205–237 (1997).
14. Bormann, J., Hamill, O.P. & Sakmann, B. Mechanism of anion permeation through channels gated by glycine and gamma-aminobutyric acid in mouse cultured spinal neurones. *J. Physiol. (Lond.)* **385**, 243–286 (1987).
15. Twyman, R.E. & Macdonald, R.L. Kinetic properties of the glycine receptor main- and sub-conductance states of mouse spinal cord neurones in culture. *J. Physiol. (Lond.)* **435**, 303–331 (1991).
16. Xu, T.L., Dong, X.P. & Wang, D.S. *N*-methyl-D-aspartate enhancement of the glycine response in the rat sacral dorsal commissural neurons. *Eur. J. Neurosci.* **12**, 1647–1653 (2000).
17. Zhu, L., Krnjevic, K., Jiang, Z., McArdle, J.J. & Ye, J.H. Ethanol suppresses fast potentiation of glycine currents by glutamate. *J. Pharmacol. Exp. Ther.* **302**, 1193–1200 (2002).
18. Fucile, S., De Saint Jan, D., de Carvalho, L.P. & Bregestovski, P. Fast potentiation of glycine receptor channels of intracellular calcium in neurons and transfected cells. *Neuron* **28**, 571–583 (2000).
19. Stelzer, A. & Wong, R.K. $GABA_A$ responses in hippocampal neurons are potentiated by glutamate. *Nature* **337**, 170–173 (1989).
20. Baker, D.A., Xi, Z.X., Shen, H., Swanson, C.J. & Kalivas, P.W. The origin and neuronal function of *in vivo* nonsynaptic glutamate. *J. Neurosci.* **22**, 9134–9141 (2002).
21. Nyitrai, G., Kekesi, K.A. & Juhasz, G. Extracellular level of GABA and Glu: *in vivo* microdialysis-HPLC measurements. *Curr. Top. Med. Chem.* **6**, 935–940 (2006).
22. Vogt, K.E. & Nicoll, R.A. Glutamate and gamma-aminobutyric acid mediate a heterosynaptic depression at mossy fiber synapses in the hippocampus. *Proc. Natl. Acad. Sci. USA* **96**, 1118–1122 (1999).
23. Barbour, B. & Hausser, M. Intersynaptic diffusion of neurotransmitter. *Trends Neurosci.* **20**, 377–384 (1997).
24. Stafford, M.M., Brown, M.N., Mishra, P., Stanwood, G.D. & Mathews, G.C. Glutamate spillover augments GABA synthesis and release from axodendritic synapses in rat hippocampus. *Hippocampus* **20**, 134–144 (2009).
25. Windhorst, U. On the role of recurrent inhibitory feedback in motor control. *Prog. Neurobiol.* **49**, 517–587 (1996).
26. Turrigiano, G. Homeostatic signaling: the positive side of negative feedback. *Curr. Opin. Neurobiol.* **17**, 318–324 (2007).
27. Hartmann, K., Bruehl, C., Golovko, T. & Draguhn, A. Fast homeostatic plasticity of inhibition via activity-dependent vesicular filling. *PLoS ONE* **3**, e2979 (2008).
28. Grillner, S. The motor infrastructure: from ion channels to neuronal networks. *Nat. Rev. Neurosci.* **4**, 573–586 (2003).
29. Clements, J.D., Lester, R.A., Tong, G., Jahr, C.E. & Westbrook, G.L. The time course of glutamate in the synaptic cleft. *Science* **258**, 1498–1501 (1992).
30. Otis, T.S., Wu, Y.C. & Trussell, L.O. Delayed clearance of transmitter and the role of glutamate transporters at synapses with multiple release sites. *J. Neurosci.* **16**, 1634–1644 (1996).
31. Bergles, D.E., Diamond, J.S. & Jahr, C.E. Clearance of glutamate inside the synapse and beyond. *Curr. Opin. Neurobiol.* **9**, 293–298 (1999).

ONLINE METHODS

All animals used in the study were housed, cared for and used experimentally in accordance with the guidelines on the ethical use of animals set forth by the Canadian Council for Animal Care and approved by the University of British Columbia Animal Care Committee.

Neuronal culture. Cultured spinal cord neurons were prepared from the lumbar spinal cords of day 14–16 fetal Wister rats. Tissues were digested with a 0.25% trypsin solution (wt/vol, Invitrogen) for 25 min at 37 °C and then mechanically dissociated using a fire-polished Pasteur pipette. The cell suspension was then centrifuged at 2,500*g* for 50 s and the cell pellets were resuspended in DMEM containing 10% fetal bovine serum (vol/vol, Sigma-Aldrich). Cells were seeded onto poly-D-lysine–coated 24-well coverslips at a density of 2.5×10^5 cells per well. Cultures were maintained in a humidified incubator with 5% CO_2 at 37 °C. After 24 h, plating medium was changed to Neurobasal medium supplemented with B-27 supplement and L-glutamine. The media were changed twice weekly thereafter. Cultured neurons were used for electrophysiological recordings 10–14 d after plating.

Slice preparation. Sprague-Dawley rats (4–6-weeks-old) were anesthetized with urethane (1.2 g per kg of body weight, intraperitoneal). The lumbar spinal cord enlargement of the spinal cord was immediately removed by a laminectomy. The dorsal and ventral roots were cut in ice-cold, oxygenated (95% O_2 and 5% CO_2) sucrose-based artificial cerebrospinal fluid (ACSF) containing 252 mM sucrose, 2.5 mM KCI, 2 mM $CaCl_2$, 2 mM $MgCl_2$, 1.25 mM KH_2PO_4, 26 mM $NaHCO_3$, 10 mM glucose and 1 mM kynurenic acid (pH 7.33–7.45, 310–330 mOsm). We cut 400-μM-thick transverse slices with a vibratome (Leica VT1000S). Before recording, the slices were incubated at 33 °C for 45 min in oxygenated normal ACSF containing 125 mM NaCl, 2.5 mM KCl, 2 mM $CaCl_2$, 1 mM $MgCl_2$, 1.25 mM NaH_2PO_4, 26 mM $NaHCO_3$ and 25 mM glucose (pH 7.4, 310–320 mOms).

HEK293 cell culture and transfection. HEK293 cells were cultured in MEM (Invitrogen) supplemented with 10% fetal bovine serum. Cells were grown to 40–60% confluence and transiently transfected using Lipofectamine 2000 (Invitrogen) according to the manufacturer's protocols. Cells were transfected with cDNA constructs encoding human GlyR α_1 or α_1 and β subunits. The constructs were subcloned into the pBK-CMV NB-200 expression vector[32]. To enhance the expression of functional heteromeric α1β GlyRs, we transfected α1 and β plasmids at a 1:40 ratio[33]. pcDNA3-GFP was also co-transfected along with GlyR subunits as a transfection marker to facilitate the visualization of the transfected cells during electrophysiological experiments. Cells were re-plated on glass coverslips 6–8 h following transfection and cultured for an additional 15–24 h before whole-cell patch-clamp recordings.

Whole-cell patch-clamp recordings. For cultured spinal neurons and HEK 293 cells, whole-cell recordings were performed under voltage-clamp mode using an Axopatch 200B or one-dimensional patch-clamp amplifier (Molecular Devices). Whole-cell currents were recorded at a holding potential of −60 mV and signals were filtered at 2 kHz and digitized at 10 kHz (Digidata 1322A). Recording pipettes (3–5 MΩ) were filled with the intracellular solution that contained 140 mM CsCl, 10 mM HEPES, 4 mM Mg-ATP and 5 mM QX-314 (pH 7.20, osmolarity, 290–295 mOsm). BAPTA (10 mM) was added in the intracellular solution (otherwise specified). The coverslips were continuously superfused with the extracellular solution containing 140 mM NaCl, 5.4 mM KCl, 10 mM HEPES, 1.0 mM $MgCl_2$, 1.3 mM $CaCl_2$ and 20 mM glucose (pH 7.4, 305-315 mOsm). To record glycinergic mIPSCs and glycine-evoked postsynaptic currents in cultured neurons, we added bicuculline (10 μM), CNQX (10 μM) and TTX (0.5 μM) to the extracellular solution to block $GABA_A$ receptors, ionotropic glutamate receptors and voltage-gated sodium channels, respectively. To evoke GlyR-mediated currents, we placed a glass pipette filled with glycine (100 μM in the Ca^{2+}-free extracellular solution) near neurons under recording. Pressure pulses (30 psi; 20–60-ms duration) were delivered to eject glycine via a Picospritzer at 30-s or 60-s intervals. To evoke glycine currents in HEK293 cells, we used fast perfusion of glycine and/or glutamate-like ligands with a computer-controlled multibarrel fast perfusion system (Warner Instruments). Maximum currents (I_{max}) were evoked by 1 mM glycine. HEK293 cells were co-transfected with homomeric α1 GlyRs unless otherwise specified. For experiments of bath perfusion of glutamate, AMPA and NMDA, 5 mM EGTA was added into Ca^{2+}-free extracellular solution unless specified elsewhere. All experiments were performed at ~22 °C.

For most experiments, spinal slices were transferred to the recording chamber and continuously superfused with oxygenated ACSF at 22–24 °C. In some experiments, slices were superfused with oxygenated ACSF at 30–32 °C. Recording pipettes filled with a CsCl-based intracellular solution had resistances of 5–7 MΩ. Whole-cell voltage-clamp recordings were made from in lamina I or II neurons at a holding potential of −65 mV[34]. Glycinergic sIPSCs were isolated by addition of 10 μM CNQX, 15 μM MK-801 and 10 μM bicuculline in the extracellular solution. Additional TTX (0.5 μM) was added into the extracellular solution to isolate glycinergic mIPSC.

Single-channel analysis. Single-channel currents were recorded in on-cell attached or outside-out patch configurations with thick-wall glass pipettes whose tips were fire-polished and coated with Sylgard. The electrodes had resistances of 6–10 MΩ. In the outside-out mode, the recording pipettes were filled with the intracellular solution and the patches were held at −60 mV. In the on-cell attached mode, the recording pipettes were filled with the extracellular solution at V_p of 0 mV. Signals were filtered at 1 kHz, sampled at 10 kHz and analyzed off-line with QuB[35,36] and Clampfit 9.0 software. An idealized recording of the durations and amplitudes of detectable events of the single-channel data was generated using 50% threshold crossing criteria. Events with a duration less than 300 μs were ignored. Bursts were defined as openings separated by closed time duration equal to or greater than a critical time (τ_c) that separated groups of openings[37]. Dwell time distributions were constructed and fitted with a mixture of exponential functions. The amplitude histograms were created and fitted with Gaussian functions. Single-channel activities were expressed as the product of the number of channels × the open probability (P_o); that is,

$$NP_o = \sum \frac{\text{open time} \times \text{number of channels open}}{\text{total time of record}}.$$

Data analysis. Values are expressed as mean ± s.e.m. (n = number of cells). One-way ANOVA or a two-tailed Student's test was used for statistical analysis and P values less than 0.05 were considered to be statistically significant. Dose-response curves were created by fitting data to the Hill equation: $I = I_{max}/(1 + EC_{50}/[A]^n)$, where I is the current, I_{max} is the maximum current, [A] is a given concentration of agonist and n is the Hill coefficient.

Chemicals. NMDA, AMPA, AP5, CNQX, NBQX, kynurenic acid, quisqualic acid, kainic acid, MK-801, YM-298198 and MPEP were purchased from Tocris. Glutamate, aspartic acid and strychnine were purchased from Sigma-Aldrich. Bicuculline methobromide was purchased from Alexis Biochemicals. TTX was purchased from Almone Labs.

32. Caraiscos, V.B. *et al.* Insulin increases the potency of glycine at ionotropic glycine receptors. *Mol. Pharmacol.* **71**, 1277–1287 (2007).
33. Burzomato, V., Groot-Kormelink, P.J., Sivilotti, L.G. & Beato, M. Stoichiometry of recombinant heteromeric glycine receptors revealed by a pore-lining region point mutation. *Receptors Channels* **9**, 353–361 (2003).
34. Chéry, N., Yu, X.H. & de Koninck, Y. Visualization of lamina I of the dorsal horn in live adult rat spinal cord slices. *J. Neurosci. Methods* **96**, 133–142 (2000).
35. Qin, F., Auerbach, A. & Sachs, F. Hidden Markov modeling for single channel kinetics with filtering and correlated noise. *Biophys. J.* **79**, 1928–1944 (2000).
36. Qin, F., Auerbach, A. & Sachs, F. A direct optimization approach to hidden Markov modeling for single channel kinetics. *Biophys. J.* **79**, 1915–1927 (2000).
37. Colquhoun, D. & Sigworth, F. Fitting and statistical analysis of single-channel records. in *Single-Channel Recording* (eds. B. Sakman & E. Neher) (Plenum Press, New York, 1995).